Inorganica Chimica Acta 449 (2016) 107–118

Contents lists available at ScienceDirect

Inorganica Chimica Acta

journal homepage: www.elsevier.com/locate/ica

Research paper

CT-DNA/BSA protein binding and antioxidant studies of new binuclear Pd(II) complexes and their structural characterisation

A. Shanmugapriya [a], G. Kalaiarasi [a], P. Kalaivani [b], F. Dallemer [c], R. Prabhakaran [a,*]

[a] Department of Chemistry, Bharathiar University, Coimbatore 641 046, India
[b] Department of Chemistry, Nirmala College for Women, Bharathiar University, Coimbatore 641018, India
[c] Laboratoire Chimie Provence-CNRS, UMR7246, Université of Aix-Marseille, Campus Scientifique de Saint-Jérôme, Avenue Escadrille Normandie-Niemen, F-13397 Marseille Cedex 20, France

ARTICLE INFO

Article history:
Received 4 February 2016
Received in revised form 2 April 2016
Accepted 7 May 2016
Available online 11 May 2016

Keywords:
Palladium(II) thiosemicarbazones
Spectroscopy
X-ray crystallography
CT-DNA/BSA protein binding
Anti-oxidant activity

ABSTRACT

New palladium(II) binuclear complexes (**1**–**4**) of the type [Pd_2(Msal-Rtsc)$_2$(μ-dppm)] (R = H or CH_3 or C_2H_5 or C_6H_5) were prepared and characterised by using various spectro analytical techniques. The true coordinating nature of the ligands in the complexes was confirmed by X-ray crystallographic studies. From the X-ray crystallographic analysis, it is found that the ligands [$\mathbf{H_2L^1}$–$\mathbf{H_2L^4}$] were bound to metal as tridentate ONS donors and phosphorus atom of bridged diphenylphosphinomethane satisfied the fourth coordination site in both the metal units to form a binuclear complexes. The interaction mode of the complexes (**1**–**4**) with calf-thymus DNA (CT-DNA) has been explored by absorption titrations and ethidium bromide displacement study was used to confirm the mode of binding. Based on the results obtained, electrostatic and intercalative binding modes have been proposed. Quenching the tryptophan and tyrosine residues of Bovine Serum Albumin (BSA) by complexes were found as static. Anti-oxidant properties of the complexes were tested against, 2,2′-diphenyl-1-picrylhydrazyl radical (DPPH), superoxide anion radicals.

1. Introduction

The chemistry of thiosemicarbazone complexes of the transition metal ions has been receiving significant current attention, largely because of their bioinorganic importance [1–7] and wide range of medicinal applications owing to their potentially beneficial biological and pharmaceutical activities such as antibacterial, antimalarial, antiviral, antitumor, anti-proliferative, antifungal, anti-inflammatory, anticonvulsant, antitubercular, antioxidant effects and inhibition of tumour growth [8–25]. These activities are due to their ability to form chelates with metals causing drastic change in the biological properties. They are well known chelating ligands coordinating to the metal ion and their coordination behaviour has been established elsewhere [26–32]. Apart from the biological properties, most of the thiosemicarbazone derivatives are used as chemical intermediates, perfume bases, dyes, rubber accelerators and liquid crystals for electronics and ion sensing ability [33,34]. Binuclear d^8 complexes have considerable attention due to their novel structural and solid state properties [35]. Among the d^8 complexes, palladium in its radioactive isotope ^{103}Pd has been used in the treatment of rapidly growing high grade prostate cancer [36,37]. Palladium(II) complexes are most probably involves in the inhibition of ribonucleotide reductase, by converting ribonucleotide to deoxyribonucleotide [38,39] and were screened against the replication of wide-type herpes simplex virus (HSV-1) and (HSV-2) strains [40]. Recently, phosphine chemistry has gained attention due to the tremendous applications in organometallic and coordination chemistry [41,42]. Bis(diphenylphosphino) methane induces unusual cyclometalation of thiophene and phenyl rings at the C2 carbon of thiosemicarbazone in Ru(II) complexes [43]. Bis(diphenylphosphino)methane containing silver(I) complexes were assayed for their antibacterial activity against two gram positive bacterial strains (*Bacillus subtilis* ATCC 6633 and Staphylococcus aureus ATCC 6538) and two gram negative bacterial strains (*Pseudomonas aeruginosa* ATCC 13525 and *Escherichia coli* ATCC 35218) [44]. Bis(diphenylphosphino)methane complexes of platinum were found to have strong anticancer activity and weak denaturing effect against albumin proteins [45]. Cyclometalated organoplatinum(II) complexes containing bisphosphine shown to have *in vitro* and *in vivo* antitumor activities [46]. Diphenylphosphinomethane ruthenium(II) arene complexes found to exhibit high chemoselectivity in the hydrogenation of aldehydes [47]. The interaction of transition metal complexes with DNA is a

* Corresponding author. Tel.: +91 422 2428319; fax: +91 422 2422387.
E-mail address: rpnchemist@gmail.com (R. Prabhakaran).

http://dx.doi.org/10.1016/j.ica.2016.05.018
0020-1693/

vibrant area of research [48]. DNA regulates most aspects of cell life and constitutes an important drug target. Designing the complexes that can bind and react with selective nucleotide sequences are of great importance in probing biological processes and in developing therapeutic drugs. An advantage of using transition metal complexes in such studies can be suited individual applications by conveniently varying their ligands and metal ions. A variety of palladium complexes are found to be effective in various therapeutic applications [49,50]. In this article, we are reporting CT-DNA/BSA (Bovine Serum Albumin)-protein binding and antioxidant studies of new binuclear palladium(II) complexes and their structural characterisation.

2. Results and discussion

2.1. Synthesis of new palladium(II) complexes

The reactions of 3-methoxysalicylaldehyde-4(N)-substituted thiosemicarbazones (**H_2L^1-H_2L^4**) with $K_2[PdCl_4]$ and 1,1′-bis (diphenylphosphino)methane [dppm] in 1:1 methanol-dichloromethane resulted in the formation of new complexes (**1–4**) (Scheme 1), the analytical data of which confirmed their stoichiometry (**1–4**). The complexes are soluble in common organic solvents such as dichloromethane, chloroform, ethanol, methanol, dimethylformamide and dimethylsulphoxide.

2.2. Spectroscopic studies

The IR spectra of the ligands **H_2L^1-H_2L^4** and the corresponding complexes provided significant information about the metal ligand bonding. A strong vibration observed at 1539–1593 cm^{-1} in the ligands corresponding to $\nu_{(C=N)}$ was shifted to 1593–1596 cm^{-1} in the complexes indicating the coordination of azomethine nitrogen to palladium ion [29,51]. A broad band at 3297–3457 cm^{-1} due to the presence of —OH group in the free ligands completely disappeared in the IR spectra of the complexes (**1–4**) indicating the coordination of phenolic oxygen to palladium after deprotonation. This was further supported by the increase in the phenolic C—O stretching frequency from 1260–1275 cm^{-1} to 1299–1313 cm^{-1} [52]. A sharp band observed at 772–788 cm^{-1} corresponding to $\nu_{(C=S)}$ in the ligands was absent in the spectra of the complexes and a new band appeared at 730–734 cm^{-1} corresponding to $\nu_{(C-S)}$ indicating the coordination of thiolate sulphur atom after enolisation and subsequent deprotonation [53,54]. In addition, the characteristic stretching frequencies corresponding to the presence of bis(diphenylphosphino)methane were found in the region 1436–1437 cm^{-1}, 1096–1097 cm^{-1} and 686–689 cm^{-1} [55]. The electronic spectra of palladium(II) complexes were recorded in chloroform and they displayed three to four bands in the region around 243–406 nm. The bands appeared at 243–244 nm have been assigned to intra ligand transition taking place within the ligands. The bands appeared around 298–301 nm have been assigned to ligand to metal charge transfer (LMCT) transitions and the bands at 341–406 nm have been assigned to metal to ligand charge transfer (MLCT) transitions [56]. The ^1H NMR spectra of the ligands (**H_2L^1-H_2L^4**) and the corresponding complexes (**1–4**) were recorded in DMSO and $CDCl_3$ (Figs. S1–S8). In the spectra of **H_2L^1-H_2L^4**, a singlet which appeared in the range δ 9.13–10.00 ppm has been assigned to N(2)H proton [57]. However, in the spectra of the new complexes (**1–4**), there was no resonance attributable to N(2)H, indicating the coordination of thiolate sulphur in the anionic form after deprotonation at N(2) [58]. A sharp singlet at δ 11.34–11.76 ppm corresponding to the phenolic —OH group in the free ligands was completely absent in all the new complexes confirming the involvement of phenolic oxygen in coordination. The aromatic protons corresponding to the coordinated ligands and diphenylphosphinomethane were found as multiplet at δ 6.31–7.93 ppm, and a sharp singlet corresponding to the —OCH_3 group also appeared at δ 3.60–3.70 ppm [59]. Two singlets observed at δ 8.36–8.50 and δ 8.37–9.20 ppm were assigned to azomethine and terminal —NH protons of the ligands [53]. However, a doublet was observed at δ 7.95–8.20 ppm in the complexes, to azomethine proton, may be due to the nuclear quadrupolar effect of nitrogen atom [53]. A sharp singlet observed around δ 7.45–8.17 ppm in **2** and **3** was assigned to the presence of terminal —NH protons of the ligands; however in the complex **4**, this resonance was mixed with aromatic protons. Two broad singlets were observed at δ 7.84 and δ 8.06 ppm corresponding to NH_2 protons of the **H_2L^1** indicating the magnetic non-equivalence of the protons which may be due to inter molecular hydrogen bonding [54]. However in the complex **1**, this resonance appeared as a singlet at δ 4.65 ppm and this up field shift may be due to the chelation which increases the shielding effect. Further, a doublet observed at δ 2.99 ppm in **H_2L^2** was found at and δ 2.71 ppm in the complex **2** indicating the presence of terminal CH_3 protons. A multiplet appeared at δ 3.55–3.58 ppm and δ 3.70–3.78 ppm in **H_2L^3** and **3** was assigned to the methylene protons of ethyl group [59]. Further, a triplet was also noted at δ 1.13 ppm and δ 1.11 ppm in **H_2L^3** and complex **3** corresponding to the presence of terminal CH_3 of ethyl group protons. In addition, a triplet was appeared around δ 4.79–4.82 ppm in the complexes indicating the presence of methylene protons of coordinated 1,1′-bis(diphenylphosphino) methane [60].

2.3. X-ray crystallography

In order to confirm the exact structure of the complexes, X-ray crystallographic studies were done for the new complexes (**1–3**). The ORTEP diagram and the numbering scheme of the complexes are given in Figs. 1–3. The crystallographic data, selected bond

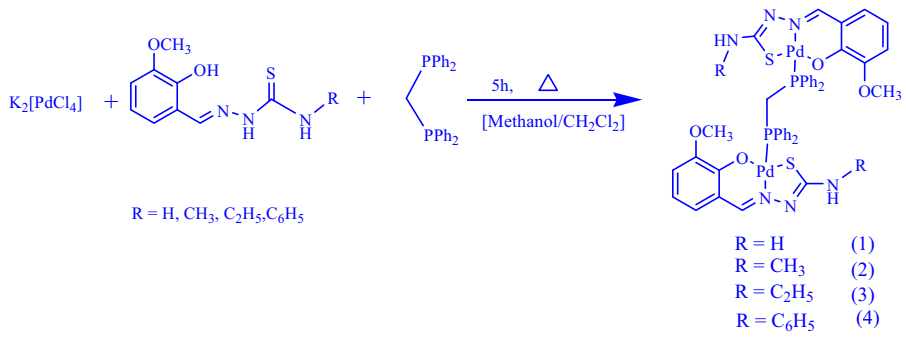

Scheme 1. Preparation of new palladium(II) complexes.

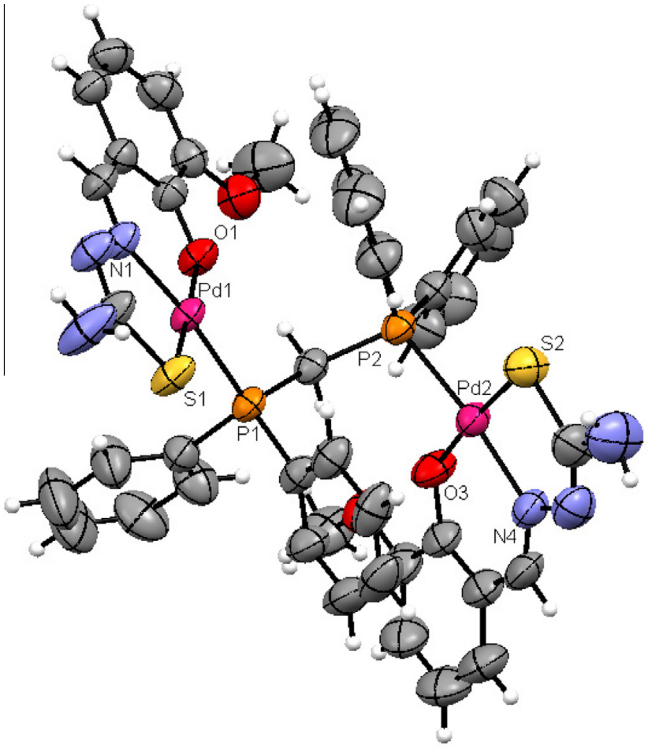

Fig. 1. ORTEP diagram of [(Pd(Msal-tsc))$_2$(μ-dppm)] (1).

distances and bond angles are listed in Tables 1 and 2. Crystallographic analysis revealed that the complexes **1–3** crystallised in monoclinic form with space group, *P*21/*c*. In the complexes (**1–3**), each palladium atom is coordinated through phenolic oxygen, N1 hydrazinic nitrogen and thiolate sulphur atom by forming a six member and five member rings. The Pd1—O1 bond distances 2.025(3) Å (**1**), 2.020(2) Å (**2**) and 2.038(3) Å (**3**) and Pd—N1 bond distances 2.018(3) Å (**1**), 2.019(2) Å (**2**) and 2.022(3) Å (**3**), and Pd1—S1 bond distances 2.245(1) Å (**1**), 2.2511(6) Å (**2**) and 2.231 (1) Å (**3**) were found as similar to the reported values [53,59,61]. The remaining binding site is occupied by the phosphorous atom of 1,1′-bis(diphenylphosphino)methane with Pd(1)—P(1) bond distances of 2.271(1) Å (**1**), 2.2775(8) Å (**2**) and 2.268(1) Å (**3**), respectively with the [S1—Pd1—N1] bite angles of 84.3(1)°, 84.01(6)° and 84.5(1)° for **1**,**2** and **3** respectively. The *trans* angles [P1—Pd1—N1] and [O1—Pd1—S1] were found as 172.4(1)°, 177.82(6)° and 176.3 (1)° for **1**,**2** and **3** respectively and 177.6(1)°, 171.67(6)° and 176.61(9)° for **1**,**2** and **3** respectively indicating the considerable deviation from the ideal symmetry and significant distortion around square planar palladium ion [61]. Two of these symmetrical units are bridged through dppm ligand in the complexes **1–3**. In complex **1**, there are two intermolecular hydrogen bonding between hydrogen atoms of terminal nitrogen (N3) and with N2 and N5 hydrazinic nitrogen atoms, forming a 2D layer structure (Fig. S9). The hydrogen bonding parameters are given in Table S1. Complex **3** exhibited an intermolecular hydrogen bonding with the oxygen atom of the water moiety which is present in the crystal lattice (Fig. S10).

2.4. DNA binding studies

DNA binding is one of the main properties in pharmacology for evaluating the anticancer property of any new compound, and hence, the interaction between DNA and metal complexes is of paramount importance in understanding the mechanism. Thus the mode and tendency for binding of complexes **1–4** to CT DNA were studied by electronic absorption and ethidium bromide (EB) displacement experiments. The interaction of transition metal complexes with DNA takes place via both covalent and/or non-covalent interaction [62]. In the case of covalent binding, the labile ligand of the complexes is replaced by a nitrogen base of DNA such as guanine N7 while the non-covalent DNA interactions include intercalative, electrostatic and groove binding of metal complexes outside of a DNA helix.

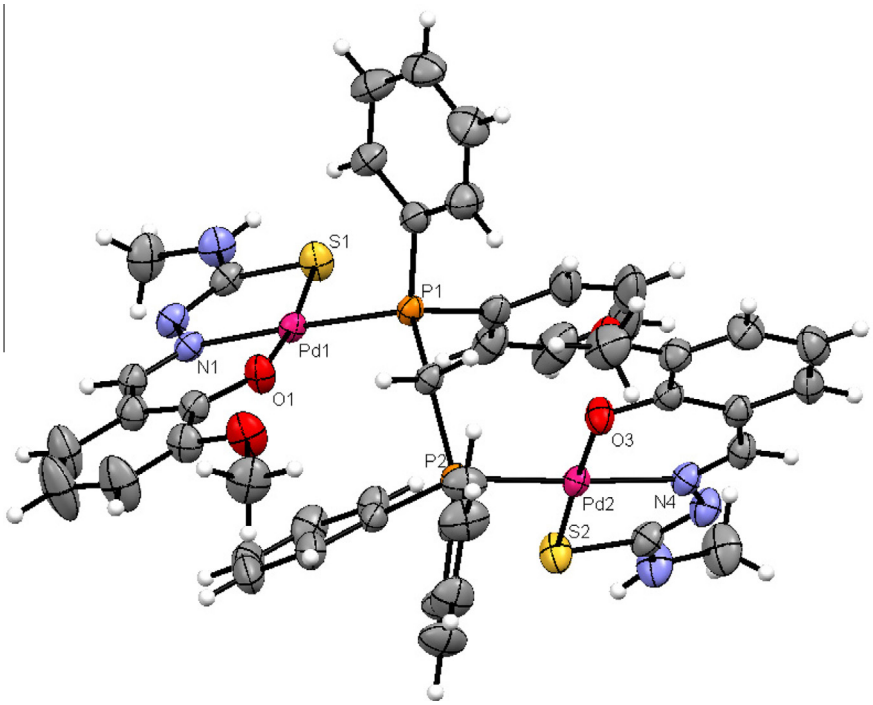

Fig. 2. ORTEP diagram of [(Pd(MSal-mtsc))$_2$(μ-dppm)] (2).

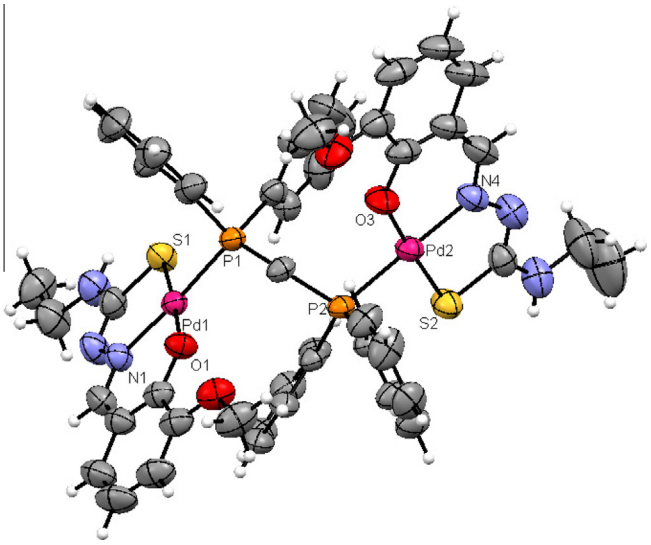

Fig. 3. ORTEP diagram of [(Pd(Msal-etsc))$_2$(μ-dppm)] (3).

2.4.1. Electronic absorption titration

Electronic absorption titration experiment was carried out to study the DNA binding properties of the new Pd(II) complexes (**1**–**4**). The absorption spectra of complexes (**1**–**4**) at a constant concentration (10 μM) in the presence of different concentrations of CT-DNA (0–50 μM) are given (Fig. 4). The absorption spectra of complex **1** mainly consist of two resolved bands [intra ligand (IL) and metal-to-ligand (MLCT) transitions] centred 246 nm (IL) and 347 nm (MLCT). While increasing the concentration DNA, a hyperchromism (A = 0.3759–0.5106) with red shift of 11 nm (up to 257) was observed in the intra ligand band. A modest hypochromism with negligible shift in the absorption maxima was found in the MLCT band at 347 nm. An isosbestic spectral change with the isosbestic point at 294 nm was observed when complex **1** binds to CT DNA. For complex **2**, upon addition of DNA, the intra ligand band at 240 nm exhibited hyperchromism (A = 0.0224–0.1549) with red shift of 4 nm was observed in the intra ligand band. The CT bands at 314, 348 and 406 nm showed hyperchromism without any shift in the absorption maxima and the binding of complex **2** to CT DNA led to isosbestic spectral change with the isosbestic point at 261 nm. Complex **3** exhibited hyperchromism (IL) at 258 nm without wavelength shift in the absorption maxima and complex **4** exhibited hyperchromism (IL) at 268 nm with a blue shift of 9 nm. The CT bands showed hypochromism at 345 nm (for **3**) and 352 nm (for **4**) without undergoing any shift upon addition of CT-DNA. The observed hyperchromic effect with red shift suggested that complexes (**1**–**4**) bind to DNA by external contact, possibly due to electrostatic binding [63]. The intrinsic binding constant K_b is a useful tool to monitor the magnitude of the binding strength of compounds with CT-DNA (Table 3). It can be determined by monitoring the changes in the absorption in the IL band at the corresponding λ_{max} with increasing concentration of DNA and is given by the ratio of the slope to the Y intercept in plots of [DNA]/($\varepsilon_a - \varepsilon_f$) versus [DNA] (Fig. 5). From the binding constant values (Table 3), it is inferred that all the complexes bind with CT-DNA efficiently. Among the four complexes, complex **4** binds more strongly with CT-DNA compared to the remaining complexes and the order of binding affinity is **1** < **2** < **3** < **4**.

2.4.2. Competitive studies with ethidium bromide

DNA binding study point out that the new palladium(II) complexes effectively bind to DNA. Further, this has been confirmed by ethidium bromide displacement experiments as done with the reported procedure [59]. The fluorescence spectra of EB were measured using an excitation wavelength of 620 nm, and the emission range was set between 550 and 750 nm. Addition of test compounds to CT DNA pre-treated with EB ([DNA]/[EB] = 1) caused reduction in the emission intensity (Fig. 6). The quenching extents of the complexes were evaluated qualitatively by employing Stern–Volmer Eq. (1). From the obtained values it is concluded that EB was replaced by the compounds from the EB-DNA system (Fig. 7 and Table 4). Such a characteristic changes is often observed in

Table 1
Crystal data and structure refinement of new Pd(II) complexes.

	[(Pd$_2$(Msal-tsc))$_2$(μ-dppm)] (**1**)	[(Pd$_2$(Msal-mtsc))$_2$(μ-ppm)] (**2**)	[(Pd$_2$(Msal-etsc))$_2$(μ-dppm)](**3**)
Empirical formula	C_{43} H_{40} N_6 O_4 P_2 Pd_2 S_2	C_{45} H_{44} N_6 O_4 P_2 Pd_2 S_2	C_{47} H_{49} N_6 O_5 P_2 Pd_2 S_2
Formula weight	1135.80	1071.72	1124.78
T (K)	293	293	293
λ (Å)	1.54184	1.54184	1.54184
Crystal system	monoclinic	monoclinic	monoclinic
Space group	$P21/c$	$P21/c$	$P21/c$
Unit cell dimension			
a (Å)	14.1487(2)	11.1101(10)	10.44070(11)
b (Å)	14.19040(17)	22.39197(10)	15.83437(12)
c (Å)	32.5313(6)	22.6748(2)	31.1277(2)
α (°)	90	90	90
β (°)	123.649(3)	128.7415	93.6697
γ (°)	90	90	90
V (Å^3)	5437.14(16)	4399.86 (9)	5135.54(8)
Z	4	4	2
Density (Mg m^{-3})	1.388	1.618	1.455
Absorption coefficient (mm^{-1})	6.980	8.585	7.405
F(000)	2304	2168	2284
Crystal size (mm)	0.16 × 0.12 × 0.06	0.16 × 0.11 × 0.07	0.02 × 0.12 × 0.08
θ range for data collection	4.42–73.67°	3.94–73.78°	3.98–73.78°
Index range	$-17 \leqslant h \leqslant 17$, $-17 \leqslant k \leqslant 17$, $-39 \leqslant l \leqslant 39$	$-13 \leqslant h \leqslant 13$, $-27 \leqslant k \leqslant 25$, $-28 \leqslant l \leqslant 27$	$-12 \leqslant h \leqslant 12$, $-19 \leqslant k \leqslant 19$, $-38 \leqslant l \leqslant 38$
Reflection collected	21796	288415	27775
Completeness to theta	66.97°	66.97°	66.97°
Refinement method	Full-matrix least-square on F^2	Full-matrix least-square on F^2	Full-matrix least-square on F^2
Data/restraints/parameters	10748/6/568	8793/0/554	10235/0/596
Goodness of fit (GOF) on F^2	1.093	1.036	1.110
Final R indices[$I > 2\sigma(I)$]	R_1 = 0.0558, wR_2 = 0.1380	R_1 = 0.0306, wR_2 = 0.0773	R_1 = 0.0487, wR_2 = 0.1163
R indices (all data)	R_1 = 0.0489, wR_2 = 0.1484	R_1 = 0.0291, wR_2 = 0.0793	R_1 = 0.0446, wR_2 = 0.1204

Table 2
Selected bond lengths (Å) and angles (°) of new Pd(II) thiosemicarbazone complexes.

	(**1**)	(**2**)	(**3**)
Bond lengths			
Pd1—O1	2.025(3)	2.020(2)	2.038(3)
Pd1—N1	2.018(3)	2.019(2)	2.022(3)
Pd1—S1	2.245(1)	2.2511(6)	2.231(1)
Pd1—P1	2.271(1)	2.2775(8)	2.268(1)
Pd2—O3	2.016(6)	2.024(2)	2.015(4)
Pd2—N4	2.023(4)	2.024(2)	2.020(5)
Pd2—S2	2.246(2)	2.2464(7)	2.254(1)
Pd2—P2	2.274(1)	2.2692(7)	2.264(1)
Bond angles			
O1—Pd1—N1	93.2(1)	93.18(8)	93.2(1)
S1—Pd1—P1	97.21(5)	96.31(3)	94.65(4)
N1—Pd1—S1	84.3(1)	84.01(6)	84.5(1)
O1—Pd1—P1	85.2(1)	86.79(6)	87.51(9)
N1—Pd1—P1	172.4(1)	177.82(6)	176.3(1)
O1—Pd1—S1	177.6(1)	171.67(6)	176.61(9)
O3—Pd2—N4	92.6(2)	93.72(8)	93.8(2)
S2—Pd2—P2	100.42(5)	99.19(3)	98.13(4)
N4—Pd2—S2	84.5(1)	83.73(6)	83.9(1)
O3—Pd2—P2	82.8(1)	83.37(6)	84.0(1)
N4—Pd2—P2	173.9(1)	176.93(6)	176.3(1)
O3—Pd2—S2	175.1(1)	177.44(6)	175.5(1)

intercalative DNA interaction [64]. Further, the apparent DNA binding constant (K_{app}) were calculated using the following equation,

$$K_{EB}\,[EB] = K_{app}[complex]$$

(where the compound concentration is the value at a 50% reduction in the fluorescence intensity of EB, K_{EB} ($1.0 \times 10^7\ M^{-1}$) is the DNA binding constant of EB, [EB] is the concentration of EB = 10 μM). The calculated values of the quenching constant (K_q) binding constant (K_{app}) are listed in Table 4. Furthermore, the observed quenching constants (K_q) and binding constants (K_{app}) of the Pd(II) complexes suggest that the interaction of all the complexes with DNA should be of intercalation [65].

2.5. Protein binding studies

The fluorescence analysis provide information on the binding mechanism, binding mode, binding constant and binding sites of small molecules to protein. The mechanism of quenching are usually classified by either dynamic quenching or static quenching. Static quenching refers to fluorophore-quencher complex formation and the dynamic quenching refers to a process in which the fluorophore and the quencher come into contact during the transient existence of the excited state.

2.5.1. UV absorption spectra of BSA

The binding of the complexes with BSA (Bovine Serum Albumin) has been estimated from the concentration dependence upon the change in the fluorescence intensity of protein after the addition of complexes. Analysing the absorption spectra of the BSA in the presence of complexes can give information about the method of quenching [66]. The UV absorption spectra of BSA in the absence and presence of four compounds showed that the (Fig. 8) absorption intensity of BSA was enhanced while adding

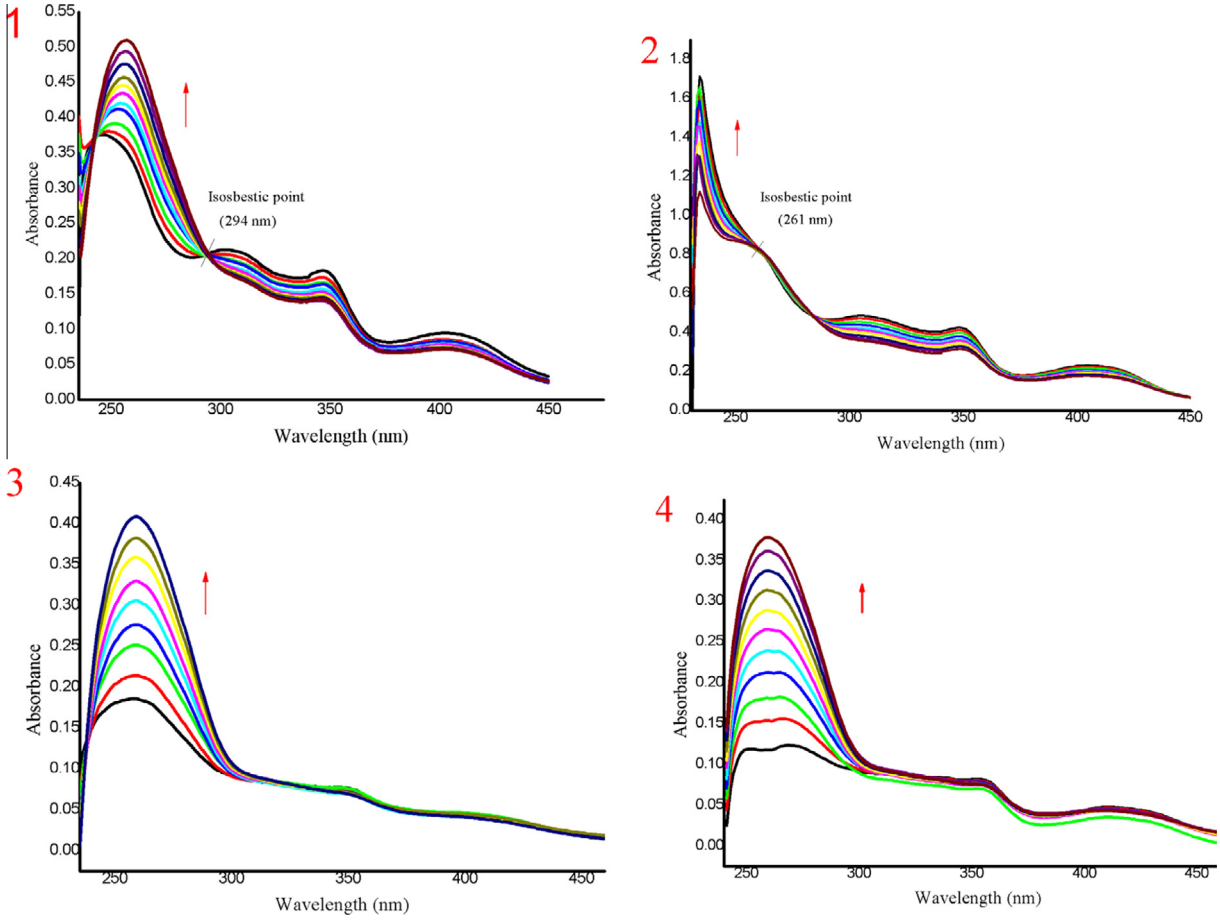

Fig. 4. Absorption titration of fixed concentration (10 μM) of complexes **1**–**4** with increasing concentrations (0–50 μM) of CT-DNA (TrisHCl buffer, pH 7).

Table 3
Binding constant for interaction of complexes with CT-DNA.

System	K_b (M^{-1})
CT-DNA + 1	3.30×10^4
CT-DNA + 2	1.89×10^5
CT-DNA + 3	4.83×10^5
CT-DNA + 4	8.71×10^5

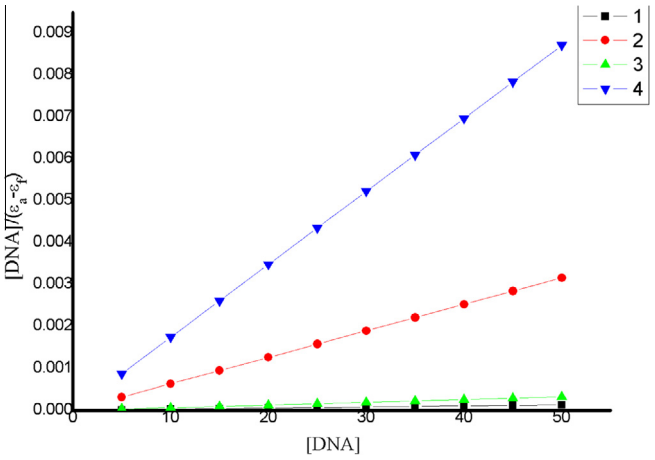

Fig. 5. Plot of [DNA] vs. [DNA]/($\varepsilon_a - \varepsilon_f$).

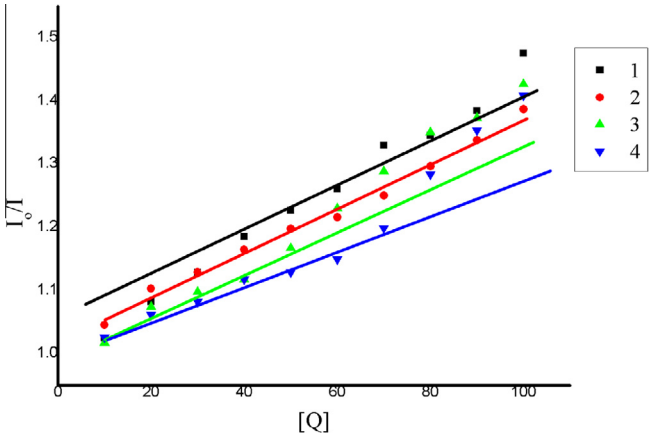

Fig. 7. Plot of [Q] vs. I_0/I.

Table 4
Quenching constant and Binding constant for interaction of complexes with DNA.

System	K_q ($\times 10^3$ M^{-1})	K_{app} ($\times 10^6$ M^{-1})
Complex 1	4.68	2.383
Complex 2	3.53	2.011
Complex 3	4.45	2.241
Complex 4	4.10	2.341

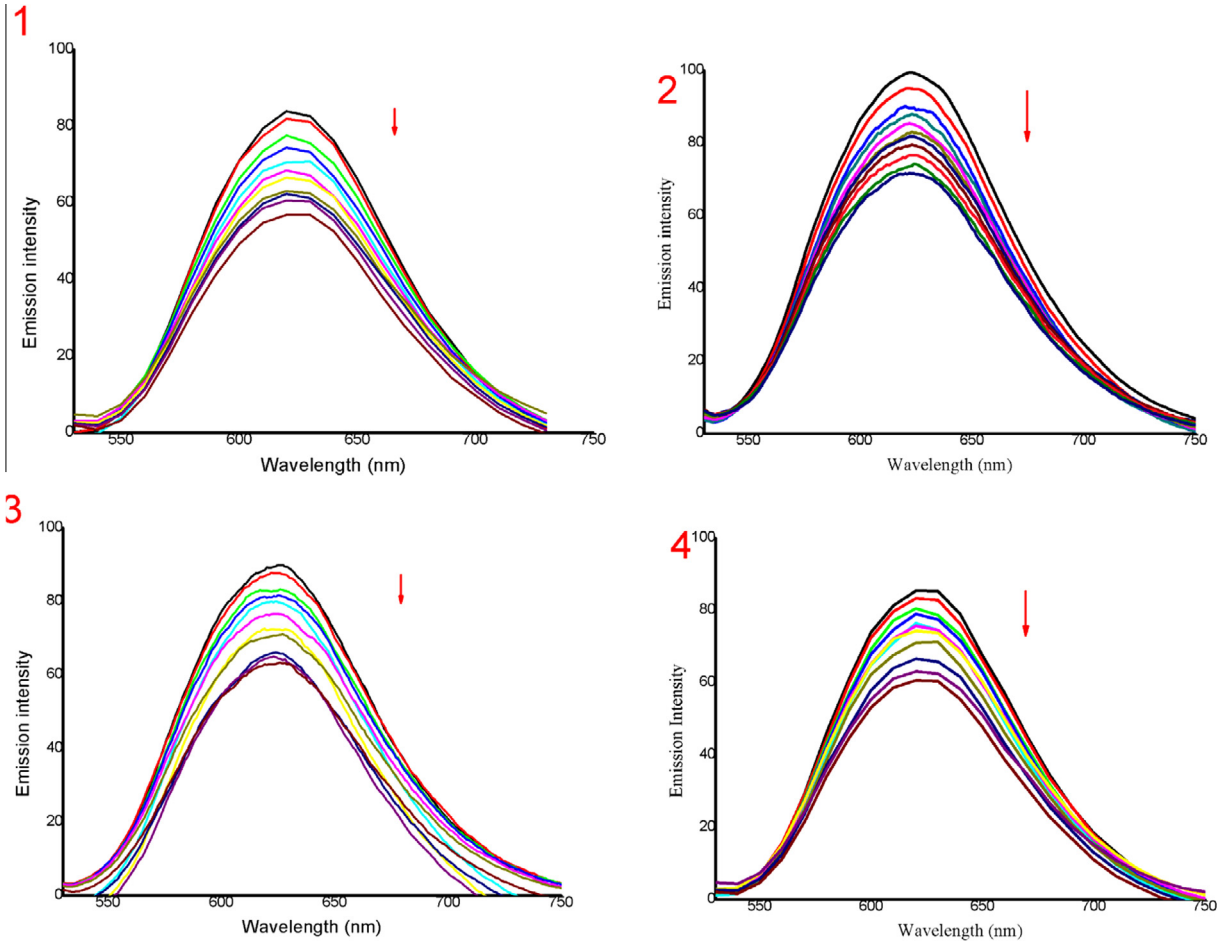

Fig. 6. Fluorescence quenching curves of ethidium bromide bound to DNA **1**–**4**. [DNA] = 10 μM, [EB] = 10 μM and [compound] = 0–100 μM.

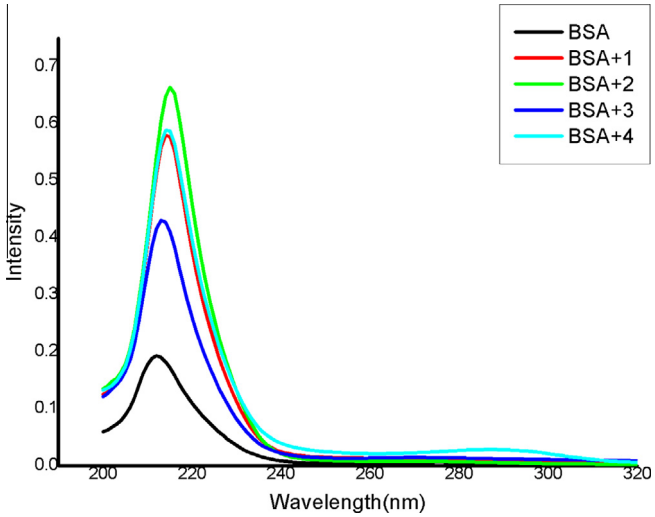

Fig. 8. UV absorption spectra of BSA (10 μM) in the presence of complexes (10 μM).

the complexes with a blue shift of 3 nm. The changes in the absorption spectra of fluoropore + quencher complex indicate the interaction of complexes with BSA. It is well known that dynamic quenching only affects the excited state of fluorophore and does not change the absorption spectrum. However, the formation of non-fluorescence ground state complex induced the change in absorption spectrum of fluorophore. Thus, possible quenching mechanism of BSA by complexes was found as static quenching [67].

2.5.2. Fluorescence quenching studies of BSA

In order to get more insight into the binding affinity of the complexes with BSA, emission titrations were done with BSA and increasing concentrations of test complexes. Among the three fluorophores, namely, tryptophan, tyrosine, and phenylalanine in BSA, the intrinsic fluorescence is mainly due to tryptophan alone, because phenylalanine has a very low quantum yield and the fluorescence of tyrosine is almost quenched when it becomes ionised or near to an amino group, a carbonyl group, or a tryptophan residue [68]. Changes in the emission spectra of tryptophan are common in response to protein conformational transitions, subunit associations, substrate binding, or denaturation. Hence, the interaction of BSA with compounds was studied by fluorescence measurement at room temperature and the binding constants of the compounds were calculated. On increasing the concentration of complexes, a progressive decrease in the fluorescence intensity was observed, accompanied with a blue shift (Fig. 9). The observed blue shift may be due to the binding of compounds with the active sites of BSA [69]. The quenching effect indicates the interaction of BSA with new Pd(II) complexes. The fluorescence quenching data have been analysed by Stern–Volmer equation.

$$I_0/I = 1 + K_{sv}[Q] \quad (1)$$

where I_0 and I are the fluorescence intensities of the fluorophore in the absence and presence of quencher, K_{sv} is the quenching constant and [Q] is the quencher concentration. A plot of I_0/I against the concentration of **1**–**4** resulted in a linear plot (Fig. 10) and the K_{sv} value is obtained from the slope. The observed linearity in the plots indicated the ability of the complexes to quench the emission intensity of BSA.

When small molecule bind to the active site of BSA, the equilibrium binding constant and the number of binding sites can be analysed by using the Scatchard Eq. (2)

$$\log[F_0 - F/F] = \log\ K + n\log[Q] \quad (2)$$

where K is the binding constant of quencher with BSA, n is the number of binding sites, F_0 and F are the fluorescence intensity in the absence and the presence of the quencher. The value of K can be determined from the slope of the plot $\log[F_0 - F/F]$ versus $\log[Q]$ (Fig. 11). The calculated value of the binding constant (K) and the number of binding sites (n) are listed in Table 5. Complex **4** has a higher magnitude of binding than other complexes. This confirms the effect of substitution on binding with BSA.

2.5.3. Synchronous fluorescence spectroscopic studies of BSA

Synchronous fluorescence spectral study was used to obtain information about the molecular environment in the vicinity of the fluorophore moieties of BSA [70]. Synchronous fluorescence spectra show tyrosine residue of BSA only at wavelength interval $\Delta\lambda$ of 15 nm whereas tryptophan residues of BSA at $\Delta\lambda$ of 60 nm. The concentration of complexes (0–100 μM) added to BSA (10 μM) is increased, a decrease in the fluorescence intensity with blue shift in the tryptophan emission maximum is observed for all the complexes (S11). In contrast, the emission intensity of tyrosine residue increases without any change in the wavelength of emission. These observations indicate that the test compounds did not affect the microenvironment of tyrosine residue during the binding process significantly but the tryptophan microenvironment to a larger extent.

2.6. Antioxidant activity

Since the palladium complexes exhibited good DNA and protein binding affinity, it was considered worthwhile to study the antioxidant properties of these compounds. Free radicals play an important role in the inflammatory process. The compounds with possible antioxidant properties could play a crucial role against inflammation and lead to potentially effective drugs. Antioxidants that exhibit radical scavenging activity are receiving increased attention since they present interesting anticancer, anti-ageing and anti-inflammatory activities. Therefore, compounds with antioxidant properties may offer protection against rheumatoid arthritis and inflammation. The radical scavenging activities of our compound along with standards, such as ascorbic acid and butylated hydroxyl toluene (BHT) in a cell free system, have been examined with reference to DPPH (2-2′-diphenyl-1-picrylhydrazide radical (DPPH·) and hydroxyl radical (OH·). The DPPH scavenging ability of the Pd(II) complex was slightly low (Fig. 12), the ability was excellent for the other radicals when compared to the standard and their IC_{50} values are listed in Table 6.

The reducing power of the complexes increases with increase in the concentration of complexes (20–100 μg/ml), and the absorbance values 0.289, 0.288, 0.283 and 0.267 nm was shown at 100 μg/ml concentration of the complexes **1**, **2**, **3** and **4** respectively are shown (Fig. 13). The complex **1** has higher activity when compared to the other complexes. The superoxide anion radical activity of the complexes increased with increasing the concentration of the complexes (Fig. 14). It is seen from the results that complexes **1**–**4** possess significant antioxidant activity. The total antioxidant activities of new palladium complexes were also assessed by phosphor molybdenum method [71] and the values are listed in Table 7. Among the four complexes, complex **4** showed the best activity.

3. Conclusion

Four new binuclear palladium(II) complexes have been synthesized and characterised by various spectro and analytical technique. The structure of the complexes 1,2, and 3 were confirmed by X-ray crystallographic studies and form the studies it is found

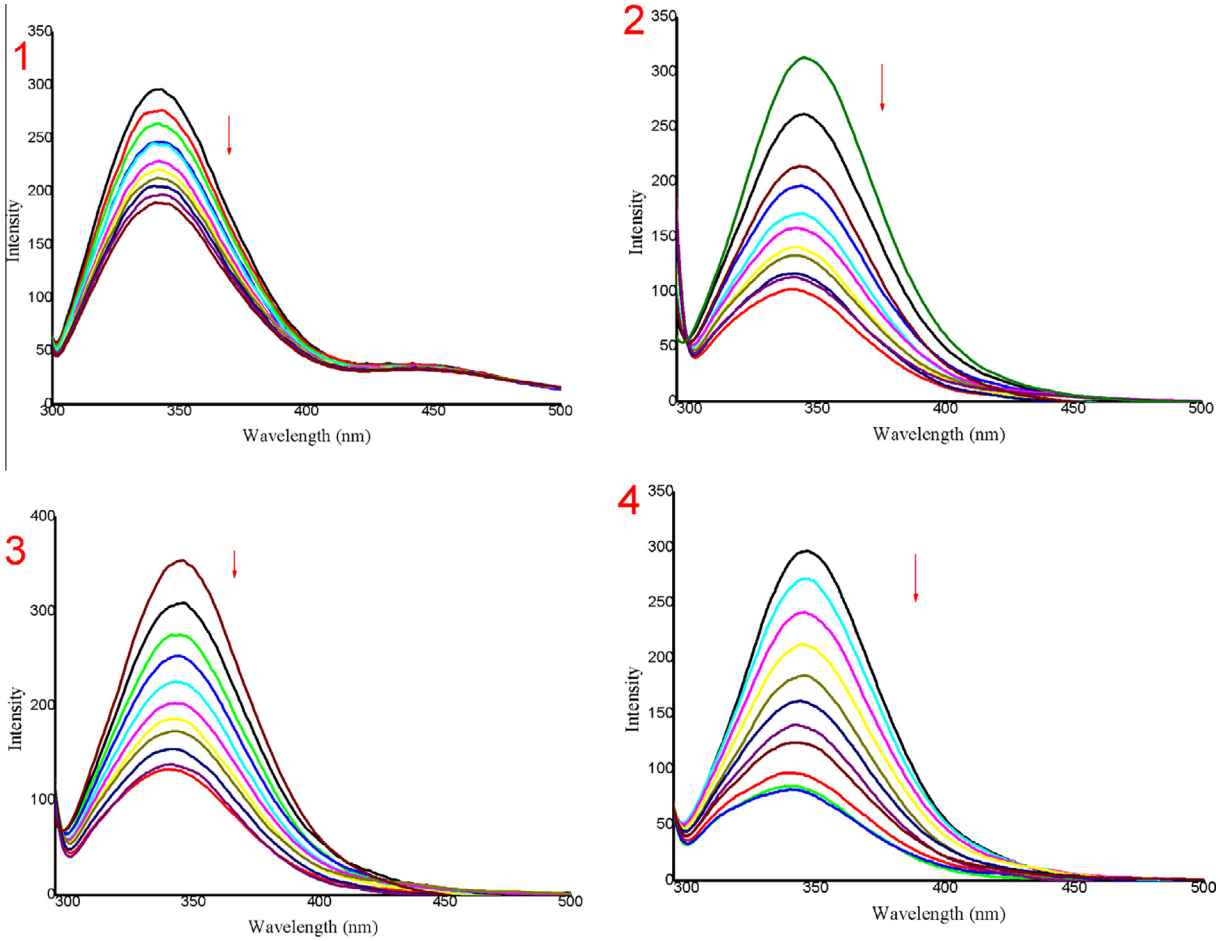

Fig. 9. Fluorescence quenching of BSA (1×10^6 M; λ_{exi} = 276; λ_{emi} = 346 nm) in the absence and presence of various concentration of complexes (0–100 μM).

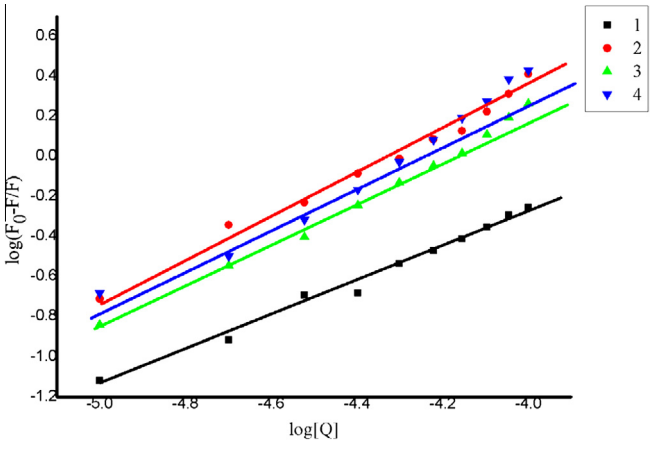

Fig. 10. Plot of [Q] vs. I_0/I.

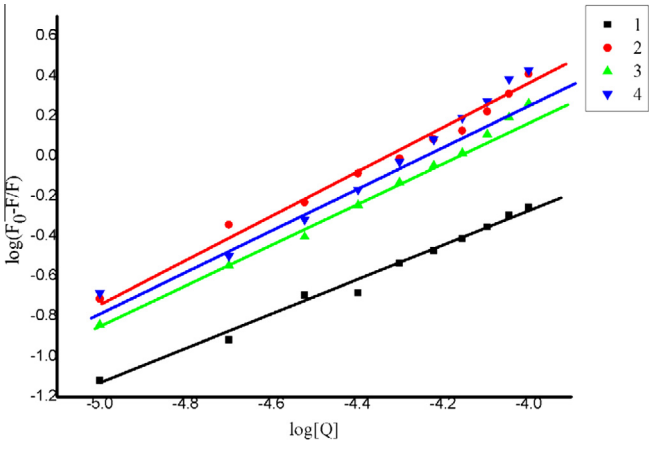

Fig. 11. Plot of log [Q] vs. log ($F_0 - F/F$).

that the ligand coordinated with metal as ONS tridentate bibasic donor. From the results of DNA binding studies, it is concluded that the complexes exhibited significant binding affinity by showing electrostatic binding mode. Whereas, the complexes quench the fluorescence of BSA by forming quencher + fluorophore complex by static quenching mechanism and thus made significant conformational change to the protein structure. The complexes exhibited significant anti oxidant activity by showing some degree of radical scavenging ability with the tested radicals.

4. Experimental

4.1. Synthesis and characterisation

1,1′-bis(diphenylphosphino)methane was purchased from Sigma Aldrich Ltd, $PdCl_2$ was purchased from Thomas Baker and CT-DNA, EB and BSA were obtained from Himedia. The ligands [$\mathbf{H_2L^1}$-$\mathbf{H_2L^4}$] and palladium complexes $K_2[PdCl_4]$ were synthesized according to the standard literature procedures [72–74]. All the

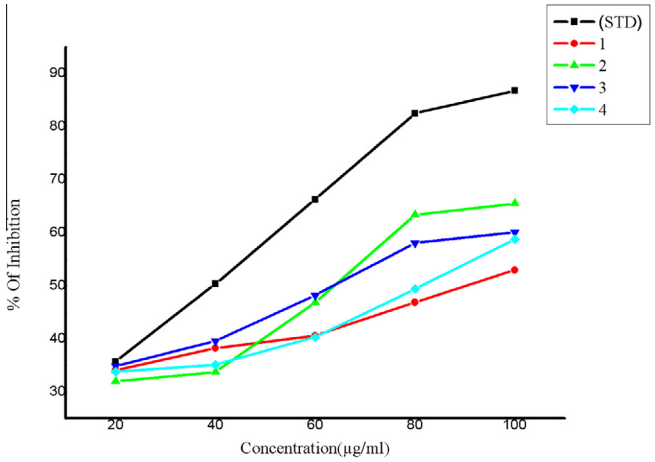

Fig. 12. DPPH scavenging activity of the new Pd(II) complexes (**1–4**).

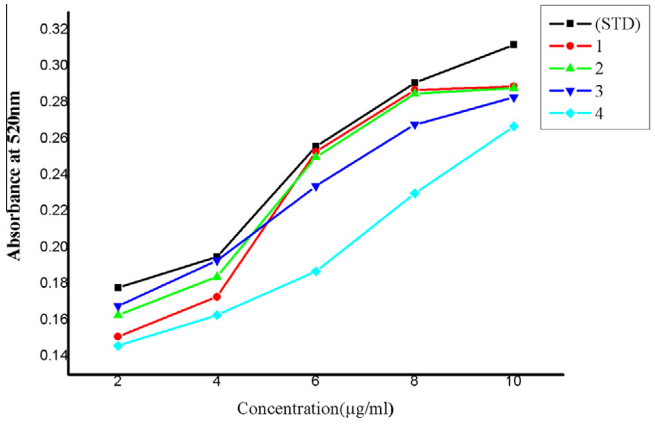

Fig. 13. Hydroxyl scavenging activity of the new Pd(II) complexes (**1–4**).

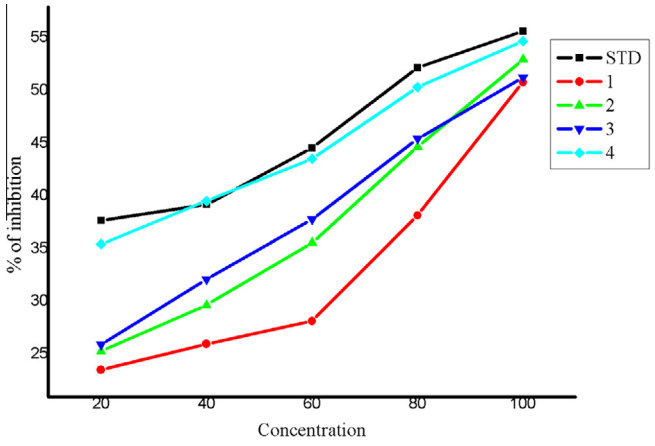

Fig. 14. Superoxide scavenging activity of new Pd(II) complexes (**1–4**).

Table 5
Quenching constant (K_{sv}), binding constant (K) and number of binding sites (n) for interaction of complexes (**1–4**) with BSA.

System	K_q (M^{-1})	K_b (M^{-1})	n
BSA + 1	5.40×10^3	1.719×10^3	0.876
BSA + 2	2.42×10^2	3.470×10^4	1.050
BSA + 3	1.83×10^2	3.908×10^4	1.094
BSA + 4	2.79×10^2	1.115×10^5	1.169

Table 6
The radical scavenging activity of the compounds.

Compounds	IC_{50} values (µM)	
	DPPH·	O_2^-
Standard	39.26	43.44
1	39.70	27.74
2	63.26	42.26
3	44.68	35.34
4	40.23	34.15

Table 7
Estimation of total antioxidant capacity of new Pd(II) complexes.

Sample	µg Ascorbic acid equivalents/ml
1	52
2	25
3	70
4	89

reagents used were analar grade, were purified and dried according to the standard procedure [75]. Infrared spectra were measured as KBr pellets on a JASCO FT-IR 4100 instrument between 400 and 4000 cm^{-1}. The electronic spectra of the complexes have been recorded in chloroform using a JASCO V-630 spectrophotometer in the 200–800 nm range. Emission spectra were recorded by using a JASCO FP 6600 spectrofluorometer.^{1}H NMR spectra were recorded in $CDCl_3$ and DMSO at room temperature with Bruker 400 MHz instrument, chemical shift relative to tetramethylsilane. Melting points were measured in a Labindia apparatus. Single crystal data collection and correction for the new Pd(II) complexes **1–3** were done at 293 K with CCD kappa diffractometer using graphite mono chromated Mo Kα (λ = 1.54184 Å) radiation [76]. The structural solution were done by using SHELXTL-97 [77] and refined by full matrix least square on F^2 using SHELXTL-97 [78].

4.2. Preparation of new palladium(II) complexes

4.2.1. Preparation of [Pd_2(Msal-tsc)$_2$(μ-dppm)] (**1**)

0.081 g of 3-methoxysalicyaldehyde thiosemicarbazone [H_2-Msal-tsc] (0.3063 mmol) was dissolved in dichloromethane (30 cm^3) and added to $K_2[PdCl_4]$ (0.100 g, 0.3063 mmol) in hot methanol (30 cm^3). The mixture was refluxed for 10 min. To this 0.058 g of 1,1′-bis(diphenylphosphino)methane (0.1531 mmol) was added. After 5 h refluxing, the reaction mixture was allowed to stand for 3 days at room temperature. A reddish brown solid formed was filtrated, washed with petroleum ether (60–80 °C) and recrystallized from toluene and methanol to yield orange red crystals. Yield: 59%, M.p. 146 °C. FT-IR (cm^{-1}) in KBr: 1596 ($\nu_{C=N}$), 1299 (ν_{C-O}), 734 (ν_{C-S}), 1437, 1096, 689 cm^{-1} (for $PPh_2(CH_2)PPh_2$); UV–Vis ($CHCl_3$), λ_{max} (nm): 243 nm (intra-ligand transition); 298 nm (LMCT); 342, 401 nm (MLCT); ^{1}H NMR ($CDCl_3$, ppm): δ 4.60 (s, 2H, NH_2), δ 7.95 (d (J = 12.8 Hz), 1H, CH = N), δ 3.64 (s, 3H, OCH_3), δ 6.31–7.85 (m, aromatic), δ 4.82 (t, 2H, CH_2).

The very similar method was followed to synthesize other complexes.

4.2.2. Preparation of [Pd_2(Msal-mtsc)$_2$(μ-dppm)] (2)

The complex **2** was prepared by the procedure as used for **1**, with 3-methoxysalicylaldehyde-4(N)-methylthiosemicarbazone [H_2-Msal-mtsc] (0.085 g, 0.3063 mmol), $K_2[PdCl_4]$ (0.100 g, 0.3063 mmol) and 1,1′-bis(diphenylphosphino)methane (0.058 g, 0.1531 mmol). Yield: 60%, M.p.206 °C. FT-IR (cm^{-1}) in KBr: 1593 ($\nu_{C=N}$), 1311 (ν_{C-O}), 732 (ν_{C-S}), 1437, 1097, 689 cm^{-1} (for $PPh_2(CH_2)PPh_2$); UV–Vis ($CHCl_3$), λ_{max} (nm): 244 nm (intra-ligand transition); 301 nm (LMCT); 342, 397 nm (MLCT); ^{1}H NMR

(DMSO-d_6, ppm): δ 7.45 (s, 1H, $NHCH_3$), δ 8.07 (d (J = 14 Hz), 1H, CH=N), δ 3.60 (s, 3H, OCH_3), δ 6.42–7.85 (m, aromatic), δ 2.71 (d (J = 4.4 Hz), 3H, CH_3), δ 4.82 (t, 2H, CH_2).

4.2.3. Preparation of $[Pd_2(Msal\text{-}etsc)_2(\mu\text{-}dppm)]$ (**3**)

The complex **3** was prepared by the procedure as used for **1**, with 3-methoxysalicylaldehyde-4(N)-ethylthiosemicarbazone [H_2-Msal-etsc] (0.090 g, 0.3063 mmol), $K_2[PdCl_4]$ (0.100 g, 0.3063 mmol) and 1,1′-bis(diphenylphosphino)methane (0.058 g, 0.1531 mmol). Yield: 52%, M.p. 164 °C. FT-IR (cm^{-1}) in KBr: 1592 ($\nu_{C=N}$), 1310 (ν_{C-O}), 733 (ν_{C-S}), 1437, 1097, 686 cm^{-1} (for $PPh_2(CH_2)PPh_2$); UV–Vis ($CHCl_3$), λ_{max} (nm): 243 nm (intra-ligand transition); 300 nm (LMCT); 343, 400 nm (MLCT); ^{1}H NMR (DMSO-d_6, ppm): δ 8.17 (s, 1H, NHC_2H_5), δ 8.05 (d (J = 13.6 Hz), 1H, CH=N), δ 3.60 (s, 3H, OCH_3), δ 6.42–7.72 (m, aromatic), δ 3.70–3.78 (m, 2H, CH_2), δ 1.11 (t, 3H, CH_3), δ 4.79 (t, 2H, CH_2).

4.2.4. Preparation of $[Pd_2(Msal\text{-}ptsc)_2(\mu\text{-}dppm)]$ (**4**)

The complex **4** was prepared by the procedure as used for **1**, with 3-methoxysalicylaldehyde-4(N)-phenylthiosemicarbazone [H_2-Msal-ptsc] (0.104 g, 0.3063 mmol), $K_2[PdCl_4]$ (0.100 g, 0.3063 mmol) and 1,1′-bis(diphenylphosphino)methane (0.058 g, 0.1531 mmol). Yield: 57%, M.p. 189 °C. FT-IR (cm^{-1}) in KBr: 1593 ($\nu_{C=N}$), 1313 (ν_{C-O}), 732 (ν_{C-S}), 1436, 1097, 687 cm^{-1} (for $PPh_2(CH_2)PPh_2$); UV–Vis ($CHCl_3$), λ_{max} (nm): 243 nm (intra-ligand transition); 341, 406 nm (MLCT); ^{1}H NMR ($CDCl_3$, ppm): δ 8.20 (d (J = 13.2 Hz), 1H, CH=N), δ 3.70 (s, 3H, OCH_3), δ 6.42–7.93 (m, aromatic), δ 4.82 (t, 2H, CH_2).

4.3. DNA binding study

CT-DNA solution of various concentrations (0–50 μM) dissolved in a trisHCl (pH 7) were added to the palladium complexes **1**–**4** (10 μM dissolved in a DMSO–H_2O mixture). Absorption spectra were recorded after equilibrium at 20 °C for 10 min. The intrinsic binding constant K_b was determined using the Stern–Volmer Eq. (3) [79,80].

$$([DNA]/[\varepsilon_a - \varepsilon_f]) = [DNA]/[\varepsilon_b - \varepsilon_f] + 1/K_b[\varepsilon_b - \varepsilon_f] \quad (3)$$

The absorption coefficients ε_a, ε_f, and ε_b correspond to A_{obsd}/[DNA], the extinction coefficient for the free complexes and the extinction coefficient for the complexes in the fully bound form, respectively. The slope and intercept of the linear fit of the plot of [DNA]/[$\varepsilon_a - \varepsilon_f$] versus [DNA] give 1/[$\varepsilon_a - \varepsilon_f$] and 1/$K_b$[$\varepsilon_b - \varepsilon_f$], respectively. The intrinsic binding constant K_b can be obtained from the ratio of the slope to the intercept. It can be determined by monitoring the changes in the absorbance in the intra ligand band at the corresponding λ_{max} with increasing concentration of DNA and is given by the ratio of slope to the Y intercept in plots of [DNA]/[$\varepsilon_a - \varepsilon_f$] versus [DNA].

4.3.1. Competitive binding with ethidiumbromide [48]

In order to know the mode of attachment of CT-DNA to the complexes fluorescence quenching experiments of EB-DNA were carried out by adding 10 μL portion of 10 μM palladium(II) complexes every time to the sample containing 10 μM EB, 10 μM DNA and Tris buffer (pH 7). Before measurements, the system was shaken and incubated at room temperature for ~5 min. The emission was recorded at 530–750 nm. On the basis of the classical Stern–Volmer equation, the quenching constant has been analysed by following equation.

$$I_0/I = K_{sv}[Q] + 1 \quad (4)$$

where I_0 and I represent the emission intensities in the absence and presence of the complexes, respectively. K_{sv} is the quenching constant and [Q] is the concentration ratio of the complex. The K_{sv} values have been obtained as a slope from the plot of I_0/I versus [Q].

4.4. Bovine Serum Albumin (BSA) binding study [66]

The protein binding study was performed by tryptophan fluorescence quenching experiments using Bovine Serum Albumin (BSA, 10 μM) as the substrate in phosphate buffer (pH 7). Quenching of the emission intensity of tryptophan residues of BSA at 346 nm (excitation wavelength at 276 nm) was monitored using compound as quenchers with increasing compound concentration. Emission spectra were recorded on a JASCO FP-6600 spectrofluorometer. A 3 ml solution containing appropriate concentration of BSA (1×10^{-6} M), was titrated with successive additions of the complex. For synchronous fluorescence spectra of BSA with various concentration of complexes (0–100 μM) were obtained from 300 to 500 nm when $\Delta\lambda$ = 60 nm and from 290 to 500 nm when $\Delta\lambda$ = 15 nm. The excitation and emission slit widths were 5 and 6 nm, respectively. Fluorescence and synchronous measurements were performed by using a 1 cm quartz cell on JASCO FP-6600 spectrofluorometer.

4.5. Evaluation of antioxidant activity

4.5.1. DPPH (1,1-diphenyl-2-picryl-hydrazyl) radical scavenging assay

The potential antioxidant activity of the new complexes (**1**–**4**) was evaluated by 2,2′-diphenyl-1-picrylhydrazyl (DPPH) radical scavenging assay was determined by the szabo method [81]. DPPH free radicals are used for rapid analysis of antioxidants. While scavenging the free radicals, the antioxidants donate hydrogen and form a stable DPPH molecule. Different concentration of the complexes (20–100 μg/ml) were prepared and subjected to antioxidant tests. To 1 ml of each of the extracts, 5 ml of 0.1 mM methanol solution of DPPH was added, vortexes, followed by incubation at 27 °C for 20 min. The radical scavenging capacity was measured every 10 min using a spectrophotometer (ELICO) by monitoring the decrease in the absorbance at 517 nm.

4.5.2. Reductive ability

The reducing power of the compounds has been investigated using the Oyaizu method [82]. 1 ml of sample solution at different concentrations was mixed with 2.5 ml of phosphate buffer (0.2 mol/l, pH 6.6) and 2.5 ml of potassium ferricyanide (1%). The mixture was incubated at 50 °C for 20 min 2.5 ml of trichloroacetic acid (TCA, 10%) was added to the mixture and centrifuged at 3000 g for 10 min. The supernatant (5 ml) was mixed with 1 ml of ferric chloride (0.1%) and the absorbance was measured at 700 nm in a Spectrophotometer. Increased absorbance of the reaction mixture indicated increased reducing power.

4.5.3. Superoxide anion scavenging activity

The superoxide anion radical scavenging activity of new Pd(II) complexes were done as per the Liu method [83]. Superoxide radicals were generated in PMS-NADH systems by oxidation of NADH and assayed by the reduction of nitrobluetetrazolium (NBT). 3 ml of sample solutions at different concentrations were mixed with 1 ml of NBT (156 μM) and 1 ml of NADH (468 μM). The reaction was initiated by adding 0.1 ml of phenazinemethosulphate (PMS) solution (60 μM) to the mixture. The reaction was incubated at 25 °C for 5 min, and the absorbance at 560 nm was measured against a blank. Decreased absorbance of the reaction mixture indicates increased superoxide anion scavenging activity.

4.5.4. Estimation of Total antioxidant capacity [71]

Total antioxidant was determined by the phosphomolybdenum method followed by samples and standard (1 ml) was mixed with

2 ml of reagent solution [ammonium molybdate (4 mM), sodium phosphate (28 mM) and sulphuric acid (0.6 M)]. All the reaction mixtures were incubated at 95 °C for 90 min. The absorbance was measured at 695 nm. Total antioxidant activity was expressed as the number of equivalent of ascorbic acid (μg/ml AA).

For the above assay, all of the tests were run in triplicate and various concentrations of the compounds were used to fix a concentration at which the compounds showed in and around 50% of activity. In addition, the percentage of activity was calculated using the formula: % of suppression ratio = $[(A_0 - A_c)/A_0] \times 100$. A_0 and A_c are the absorbance in the absence and presence of the tested compounds, respectively. The 50% activity (IC_{50}) can be calculated using the percentage of activity.

Acknowledgment

Department of Science and Technology (DST-SERB)(SR/FT/CS-32-/2011 dated 04.05.2012) and Council of Science and Industrial Research (CSIR) (01(2553)/12/EMR-II dated 03.04.2012) New Delhi, India are greatly acknowledged for their financial support. The author A.S. gratefully acknowledges the University Grants Commission (UGC), New Delhi for UGC-BSR Fellowship, New Delhi, India [Grand No. G2/14308/17750/UGC BSR/Selection Comt./2014 dt.15.09.2014]. The author G.K. gratefully acknowledges the Department of Science and Technology (DST) New Delhi for INSPIRE Fellowship, New Delhi, India [IF140225 dt.23.01.2014].

Appendix A. Supplementary material

CCDC 1445118, 1445119 and 1445120 contains the supplementary crystallographic data. These data can be obtained free of charge from The Cambridge Crystallographic Data Centre via www.ccdc.cam.ac.uk/data_request/cif. Supplementary data associated with this article can be found, in the online version, at http://dx.doi.org/10.1016/j.ica.2016.05.018.

References

[1] M.J.M. Campbell, Coord. Chem. Rev. 15 (1975) 279.
[2] S.B. Padhye, G.B. Kaffman, Coord. Chem. Rev. 63 (1985) 127.
[3] I. Haiduc, C. Silvestru, Coord. Chem. Rev. 99 (1990) 253.
[4] D.X. West, A.E. Liberta, S.B. Padhye, R.C. Chikate, P.B. Sonawane, A.S. Kumbhar, R.G. Yerande, Coord. Chem. Rev. 123 (1993) 49.
[5] A.G. Quiroga, C.N. Raninger, Coord. Chem. Rev. 248 (2004) 119.
[6] T.S. Lobana, R. Sharma, G. Bawa, S. Krishna, Coord. Chem. Rev. 253 (2009) 977.
[7] A. Garoufis, S.K. Hadjikakou, N. Hadjiliadis, Coord. Chem. Rev. 253 (2009) 1384.
[8] F.A. French, E. Blanz Jr., J. Med. Chem. 13 (1970) 1117.
[9] J.P. Scovill, D.L. Klayman, C.F. Franchino, J. Med. Chem. 25 (1982) 1261.
[10] A. Kraker, S. Krezoski, J. Schneider, D. Mingel, D.H. Petering, J. Biol. Chem. 260 (1985) 13170.
[11] A.E. Liberta, D.X. West, Biometals 5 (1992) 121.
[12] D. Kovala-demertzi, A. Domopoulou, M.A. Demertzis, C.P. Raptopoulou, A. Terzis, Polyhedron 13 (1994) 1917.
[13] D. Kovala-Demertzi, J.R. Miller, N. Kourkoumelis, S.K. Hadjikakou, M.A. demertzis, Polyhedron 18 (1999) 1005.
[14] J. Patole, S. Dutta, S. Padhye, E. Sinn, Inorg. Chim. Acta 318 (2001) 207.
[15] R.I. Maurer, P.J. Blower, J.R. Dilworth, C.A. Reynolds, Y. Zheng, G.E.D. Mullen, J. Med. Chem. 45 (2002) 1420.
[16] A.R. Cowly, J.R. Dilworth, P.S. Donnely, E. Labisbal, A. Souse, J. Am. Chem. Soc. 124 (2002) 5270.
[17] M.B. Ferrari, F. Bisceglie, G. Pelosi, M. Sassi, P. Tarasconi, M. Cornia, S. Capacchi, R. Albertini, S. Pinelli, J. Inorg. Biochem. 90 (2002) 113.
[18] S. Padhye, Z. Afrasiabi, E. Sinn, J. Fok, K. Mehta, N. Rath, Inorg. Chem. 44 (2005) 1154.
[19] J. Ruiz, N. Cutillas, C. Vicente, Inorg. Chem. 44 (2005) 7365.
[20] A.A. Abeer, A.S. Shayma, A.Y. Wagee, M.A. Hapipah, A.A. Mahmood, Bull. Chem. Soc. Ethiop. 26 (1) (2012) 95.
[21] A.E. Ahmed, Inorg. Chim. Acta 362 (2009) 4991.
[22] H.M. Ali, S. Puvaneswary, W.J. Basrun, Malays. J. Sci. 25 (1) (2006) 107.
[23] V.A. Madalina, F.B. Stefania, D. Constantin, L.A. Gabriela, Eur. J. Med. Chem. 45 (2010) 2055.
[24] E.Z. Vinuelas, M.A. Maldonado, F.G. Luna, F.J. Barros, Polyhedron 27 (2008) 879.
[25] P. Chellan, K.M. Land, A. Shokar, A. Au, S. Hwan An, C.M. Clavel, P.J. Dyson, C.D. Kock, P.J. Smith, K. Chibale, G.S. Smith, Organometallics 31 (2012) 5791.
[26] F. Basuli, S.M. Peng, S. Bhattacharya, Inorg. Chem. 36 (1997) 5645.
[27] F. Basuli, S.M. Ruf, C.G. Pierpont, S. Bhattacharya, Inorg. Chem. 37 (1998) 6113.
[28] I. Pal, F. Basuli, T.C.W. Mak, S. Bhattacharya, Angew. Chem. Int. Ed. Engl. 40 (2001) 2923.
[29] R. Prabhakaran, R. Karvembu, T. Hashimoto, K. Shimizu, K. Natarajan, Inorg. Chim. Acta 358 (2005) 6093.
[30] L.M. Fostiak, I. Gracia, J.K. Swearinger, E. Bermejo, A. Castineivas, D.X. West, Polyhedron 22 (2003) 83.
[31] L. Ze-Hua, D. Chun-Ying, L. Ji-Hui, L. Young-Jiang, M. Yu-Hua, Y. Xiao-Zeng, New J. Chem. 24 (2000) 1057.
[32] S.B. Novakovi, G.A. Bogdanovic, V.M. Leovac, Inorg. Chem. Commun. 8 (2005) 9.
[33] A.A. Abeer, A.S. Shayma, A.Y. Wagee, M.A. Hapipah, A.A. Mahmood, Orient. J. Chem. 27 (4) (2011) 1437.
[34] R.K. Mahajan, I. Kaur, T.S. Lobana, Talanta 59 (2003) 101.
[35] V.K. Jain, L. Jain, Coord. Chem. Rev. 249 (2005) 3075.
[36] N.N. Stone, P.G. Stock, Eur. Urol. 41 (2002) 427.
[37] L. Potters, Y. Cao, E. Calugaru, T. Torre, P. Fearn, X.H. Wang, Int. J. Radiat. Oncol. Biol. Phys. 50 (2001) 605.
[38] E. Bermejo, R. Carballa, A. Castineiras, R. Dominguez, A.E. Liberta, C. Maichelle-Mossmer, M.M. Salberg, D.X. West, Eur. J. Inorg. Chem. (1999) 965.
[39] A.G. Quiroga, J.M. Perez, I.L. Solera, J.R. Masaguar, A. Luque, P. Roman, A. Edwaeds, C. Alonso, C.N. Ranninger, J. Med. Chem. 41 (1998) 1399.
[40] P. Genova, T. Varadinova, A.I. Matesanz, D. Marinova, P. Souza, Toxicol. Appl. Pharmacol. 197 (2004) 107.
[41] M. Batool, T.A. Martin, M.A. Naser, M.W. George, S.A. Macgregor, M.F. Mahno, M.K. Whittlesey, Chem. Commun. 47 (2011) 11225.
[42] E. Fourie, J.M.J. Rensburg, J.C. Swarts, J. Organomet. Chem. 754 (2014) 80.
[43] T.S. Lobana, G. Bawa, A. Castineiras, R.J. Butcher, M. Zeller, Organometallics 27 (2008) 175.
[44] B. Ruan, Y. Tian, H. Zhou, J. Wu, Z. Liu, C. Zhu, J. Yang, H. Zhu, J. Org. Chem. 694 (2009) 2883.
[45] R. Yousefi, S. Aghelian, F. Mokhtari, H. Samouei, M. Rashidi, S.M. Nabavizadeh, Z. Tavaf, Z. Pouryasin, A. Niazi, R. Faghihi, M.M. Papari, Appl. Biochem. Biotechnol. 167 (2012) 861.
[46] M. Frezza, Q.P. Dou, Y. Xiao, H. Samouei, M. Rashidi, F. Samari, B. Hemmateenejad, J. Med. Chem. 54 (2011) 6166.
[47] A.B. Chaplin, P.J. Dyson, Organometallic 26 (2007) 4357.
[48] (a) J. Reedijk, Chem. Rev. 99 (1999) 2499;
(b) J. Reedijk, Curr. Opin. Chem. Biol. 3 (1999) 236;
(c) Y.W. Jung, S.J. Lippard, Chem. Rev. 107 (2007) 1387.
[49] (a) A.C.F. Caires, Anti-Cancer Agents Med. Chem. 7 (2007) 484;
(b) J. Ruiz, J. Lorenzo, C. Vicente, G. Lopez, J.M. Lopez-de-Luzuriaga, M. Monge, F.X. Aviiles, D. Bautista, V. Moreno, A. Laguna, Inorg. Chem. 47 (2008) 6990;
(c) P. Starha, Z. Travnicek, L. Popa, J. Inorg. Biochem. 103 (2009) 978.
[50] (a) M. Juribanic, K. Molcanov, B. Kojic-Prodic, L. Bellotto, M. Kralj, F. Zani, L. Tunek-Bozic, J. Inorg. Biochem. 105 (2011) 867;
(b) P.I. da, S. Maia, A. Graminha, F.R. Pavan, C.Q.F Leite, A.A. Batista, D.F. Back, E. S. Lang, J. Ellena, S. de, S. Lemos, H.S.S. de. Araujo, V.M. Deflon, J. Braz. Chem. Soc. 21 (2010) 1177;
(c) S.A. Khan, M. Yusuf, Eur. J. Med. Chem. 44 (2009) 2270;
(d) L. Otero, M. Vieites, L. Boiani, A. Denicola, C. Rigol, L. Opazo, C.O. Azar, J.D. Maya, A. Morello, R.L. Krauth-Siegel, O.E. Piro, E. Castellano, M. Gonzalez, D. Gambino, H. Cerecetto, J. Med. Chem. 49 (2006) 3322.
[51] R. Prabhakaran, C. Jayabalakrishnan, V. Krishnan, K. Pasumpon, D. Sukanya, H. Bertagnolli, K. Natarajan, Appl. Organomet. Chem. 20 (2006) 203.
[52] R. Prabhakaran, P. Kalaivani, R. Jayakumar, M. Zeller, A.D. Hunter, S.V. Renukadevi, E. Ramachadran, K. Natarajan, Metallomics 3 (2011) 42.
[53] R. Prabhakaran, S.V. Renukadevi, R. Karvembu, R. Huang, J. Mautz, G. Hunter, R. Subhaskumar, K. Natarajan, Eur. J. Med. Chem. 43 (2008) 268.
[54] R. Prabhakaran, S.V. Renukadevi, R. Karvembu, R. Huang, M. Zeller, K. Natarajan, Inorg. Chim. Acta 361 (2008) 2547.
[55] R. Karvembu, S. Hemalatha, R. Prabhakaran, K. Natarajan, Inorg. Chem. Commun. 6 (2003) 486.
[56] P. Kalaivani, R. Prabhakaran, F. Dallemer, P. Poornima, E. Vaishnavi, E. Ramachadran, V. Vijay Padma, R. Renganathan, K. Natarajan, Metallomics 4 (2012) 101;
(b) P. Kalaivani, C. Umadevi, R. Prabhakaran, F. Dallemer, P.S. Mohan, K. Natarajan, Polyhedron 80 (2014) 97.
[57] T.S. Lobana, A. Sanchez, J.S. Casas, A. Castineires, J. Sordo, M.S. Garciaasende, E. M. Vazquez-Lopez, Dalton Trans. (1997) 4289.
[58] T.S. Lobana, P. Kumari, G. Hundal, R.J. Butcher, Polyhedron 29 (2010) 1130.
[59] R. Prabhakaran, P. Kalaivani, P. Poornima, F. Dalllmer, G. Paramaguru, V. Vijaya Padma, R. Renganathan, R. Hung, K. Natarajan, Dalton Trans. 41 (2012) 9323.
[60] M. Lopez-Torres, A. Fernandez, J.J. Fernandez, A. Suarez, S. Castro-Juiz, M.T. Pereira, J.M. Villa, J. Org. Chem. 665 (2002) 127.
[61] P. Chellan, N. Shunmoogam-Gounden, D.T. Hendricks, J. Gut, P.J. Rosenthal, C. Lategan, P.J. Smith, K. Chibale, G.S. Smith, Eur. J. Inorg. Chem. (2010) 3520.
[62] Q.L. Zhang, J.G. Liu, H. Chao, G.Q. Xue, L.N. Ji, J. Inorg. Biochem. 83 (2001) 49.
[63] E.C. Long, J.K. Barton, Acc. Chem. Res. 23 (1990) 271.
[64] M. Chauhan, F. Arjmand, K. Banerjee, Inorg. Chem. 46 (2007) 3072.
[65] R. Senthil Kumar, S. Arunachalam, V.S. Periasamy, C.P. Preethy, A. Riyasdeen, M.A. Akbarsh, J. Inorg. Biochem. 103 (2009) 117.
[66] Y.J. Hu, Y. Liu, J.B. Wang, X.H. Xiao, S.S. Qu, J. Pharm. Biomed. Anal. 36 (2004) 915.
[67] H.Y. Liu, Z.H. Xu, X.H. Liu, Chem. Pharm. Bull. 57 (2009) 1237.
[68] A. Sulkowska, J. Mol. Struct. 614 (2002) 227.

[69] Y. Wang, H. Zhang, G. Zhang, W. Tao, S. Tang, J. Lumin. 126 (2007) 211.
[70] N. Wang, L. Ye, B.Q. Zhao, J.X. Yu, Braz. J. Med. Res. 41 (2008) 589.
[71] P. Prieto, M. Pineda, M. Aguilar, Anal. Biochem. 269 (1999) 337.
[72] P. Kalaivani, R. Prabhakaran, E. Ramachandran, F. Dallmer, G. Paramaguru, R. Renganathan, P. Poornima, V. Vijay Padma, K. Natarajan, Dalton Trans. 41 (2012) 2486.
[73] S. Purohit, A.P. Koley, L.S. Prsad, P.T. Manoharan, S. Ghosh, Inorg. Chem. 28 (1989) 3735.
[74] Y. Guo, K. Fhayli, S. Li, Y. Yang, A. Mashat, N.M. Khashab, RSC Adv. 3 (2013) 17693.
[75] A.L. Vogel, Text Book of Practical Organic Chemistry, fifth ed., Longman, London, 1989, p. 268.
[76] (a) R.H. Blessing, Acta Crystallogr. Sect. A 51 (1995) 33;
(b) R.H. Blessing, Cryst. Rev. 1 (1987) 73;
(c) R.H. Blessing, J. Appl. Crystallogr. 22 (1989) 396.
[77] G.M. Sheldrick, SHELXTL Version 5.1. An Integrated System for Solving, Refining and Displaying Crystal Structures from Diffraction Data, Siemens Analytical X-ray Instruments, Madison WI, 1990.
[78] G.M. Sheldrich, SHELXTL-97, Program for Refinement of Crystal Structures, University of Gottingen, Germany, 1997.
[79] A. Wolfe, G.H. Shimer, T. Meehan, Biochemistry 26 (1987) 6392.
[80] G. Cohen, H. Eisenberg, Biopolymers 8 (1969) 45.
[81] M.R. Szabo, C. Idtoiu, D. Chambre, A.X. Lupea, Chem. Mater. Sci. 61 (2007) 214.
[82] M. Oyaizu, Jpn. J. Nutr. 44 (1986) 307.
[83] F. Liu, V.E.C. Ooi, S.T. Chang, Life Sci. 60 (1997) 763.